

Bimodality of circumstellar disk evolution induced by Hall current

Y. Tsukamoto^{1,2}, K. Iwasaki^{2,3}, S. Okuzumi⁴, M. N. Machida⁵, and S. Inutsuka²

¹Laboratory of Computational Astrophysics, RIKEN, Saitama, Japan

²Department of Physics, Nagoya University, Aichi, Japan

³Department of Environmental Systems Science, Faculty of Science and Engineering, Doshisha University, Kyoto, Japan

⁴Department of Earth and Planetary Sciences, Tokyo Institute of Technology, Tokyo, Japan

⁵Department of Earth and Planetary Sciences, Kyushu University, Fukuoka, Japan

15 November 2019

ABSTRACT

The formation process of circumstellar disks is still controversial because of the interplay of complex physical processes that occurs during the gravitational collapse of prestellar cores. In this study, we investigate the effect of the Hall current term on the formation of circumstellar disk using three-dimensional simulations. In our simulations, all non-ideal effects as well as the radiation transfer are considered. We show that the size of the disk is significantly affected by a simple difference in the inherent properties of the prestellar core, namely whether the rotation vector and the magnetic field are parallel or anti-parallel. In the former case, only a very small disk (< 1 AU) is formed. On the other hand, in the latter case, a massive and large (> 20 AU) disk is formed in the early phase of protostar formation. We also show that the anti-rotating envelopes against the disk-rotation appear with a size of $\gtrsim 200$ AU. We predict that the anti-rotating envelope will be found in the future observations.

Key words: star formation – circum-stellar disk – methods: hydrodynamics – smoothed particle hydrodynamics – protoplanetary disk – planet formation

1 INTRODUCTION

Circumstellar disks are born around protostars in the course of the self-gravitational collapse of the molecular cloud core. Because the disks are the formation sites of planets, the formation and the evolution processes of the disk essentially determines the initial conditions for planet formation. Understanding the disk formation requires an accurate description of the angular momentum evolution because the centrifugal force is the dominant force in opposing the gravitational force. Observations of cloud cores have shown that they have the finite angular momentum (Goodman et al. 1993). Thus, the circumstellar disk formation around very young protostar has been believed to be a natural consequence of angular momentum conservation in the gravitationally collapsing molecular cloud core. In fact, several previous studies of the disk formation without a magnetic field show that relatively large disk with a size of $r \sim 100$ AU forms during the early phase of protostar formation (e.g., Bate 1998; Tsukamoto & Machida 2011, 2013).

However, the magnetic field changes the simple picture of the disk formation. As shown by observations of the Zeeman effect, typical cloud cores are relatively strongly magnetized (Troland & Crutcher 2008). During the gravitational

collapse, a toroidal magnetic field is created by the rotation. When the magnetic field becomes sufficiently strong, the magnetic tension decelerates the gas rotation, removing the angular momentum. This effect is known as magnetic braking (Mouschovias & Paleologou 1979). Previous studies using ideal magnetohydrodynamics (MHD) simulations have shown that the magnetic braking plays an important role in the disk formation and evolution processes. The disk size decreases in response to the increase of initial magnetic field strength (Bate, Tricco & Price 2014) and, for a typical magnetic field strength, the formation of a disk is almost completely suppressed in early Class 0 phase (Mellon & Li 2008; Hennebelle & Fromang 2008).

Meanwhile, the observations of Class 0 young stellar objects (YSOs) showed that a relatively large circumstellar disk ($r \sim 50$ AU) exists around young protostars (Ohashi et al. 2014; Sakai et al. 2014). Recently, observations of a number of Class 0 YSOs in Perseus (Tobin et al. 2015) revealed that five of the nine of the observed Class 0 YSOs show the signature of a disk, while no disk signature could be observed for the remaining Class 0 YSOs. These observations indicate that some very young protostars have relatively large circumstellar disks with a size of $r > 10$ AU,

suggesting a disagreement between the previous theoretical works and the observations.

Possible physical mechanisms for resolving the discrepancy between theory and observation are the magnetic diffusions (Mellon & Li 2009; Machida & Matsumoto 2011; Machida, Inutsuka & Matsumoto 2014; Tomida, Okuzumi & Machida 2015; Tsukamoto et al. 2015a). Previous works following the formation of protostars showed that the small disk with size of $r \lesssim 1$ AU is formed around the protostar when the magnetic diffusions are considered (Machida & Matsumoto 2011; Tomida et al. 2013; Tsukamoto et al. 2015a). However, the formation of a disk with a size of $r \gtrsim 10$ AU at the early phase of protostar formation in a typically magnetized cloud core is still highly difficult even with these effects.

The effect of the Hall current term is the least studied in the context of disk formation. The Hall current term generates a toroidal magnetic field from the poloidal magnetic field and directly affects the magnetic tension that determines the magnetic braking efficiency. The Hall current term in MHD equations is not invariant against the global inversion of the magnetic field (Wardle & Ng 1999; Krasnopolsky, Li & Shang 2011; Li, Krasnopolsky & Shang 2011; Braiding & Wardle 2012) and its effect on the disk formation is different depending on whether rotation vector and magnetic field of host cloud core are parallel or anti-parallel (or, in other words, whether the rotation vector points toward the magnetic north or south pole). When the rotation vector and the magnetic field are anti-parallel, the Hall current term weakens the magnetic braking. Meanwhile, the Hall current term strengthens the magnetic braking in the parallel case. Despite the possible importance of the Hall current term in the disk evolution, it is still unclear how the Hall current term affects the formation of the circumstellar disk because the previous numerical studies (Krasnopolsky, Li & Shang 2011; Li, Krasnopolsky & Shang 2011) neglected the first core evolution phase, which plays an important role in the disk formation (Machida & Matsumoto 2011; Dapp, Basu & Kunz 2012; Tsukamoto et al. 2015a) and simplified the radiation transfer. Furthermore, they employed a relatively large inner boundary radius of $r \gtrsim 6$ AU and the gas dynamics within several times of the inner radius may be affected by the inner boundary. In other words, the disk with the radius of $r \lesssim 20$ AU would not be resolved with their inner boundary. Three-dimensional simulations are also necessary to investigate the non-axisymmetric effects such as the gravitational instability which may be important in the early phase of disk formation (Tsukamoto et al. 2015a).

In this paper, we performed three-dimensional simulations starting from prestellar molecular cloud cores. Our numerical simulations include all non-ideal MHD effects as well as the radiation transfer. The simulations were conducted until sufficiently after the birth of the protostar. We did not use any sink particle technique for the center and hence our simulations do not suffer from numerical artifacts introduced by sink particle or the inner boundary which may artificially change the formation and evolution of the disk (Machida, Inutsuka & Matsumoto 2014). The simulation models are summarized in Table 1.

2 NUMERICAL METHOD AND INITIAL CONDITIONS

In this study, we solved the non-ideal radiation magnetohydrodynamics equations with self-gravity. The numerical method, except for the Hall current term, is the same used in our previous study (Tsukamoto et al. 2015a). The ideal MHD part was solved by using the Godunov smoothed particle magnetohydrodynamics (GSPMHD) method (Iwasaki & Inutsuka 2011). The sinusoidal condition of the magnetic field $\nabla \cdot \mathbf{B} = 0$ was maintained by the hyperbolic divergence cleaning method for GSPMHD (Iwasaki & Inutsuka 2013). The radiative transfer was treated by the FLD-SPH method (Whitehouse & Bate 2004; Whitehouse, Bate & Monaghan 2005). We treated Ohmic and ambipolar diffusion with the method described by Tsukamoto, Iwasaki & Inutsuka (2013) and Wurster, Price & Ayliffe (2014), respectively. Both diffusion processes were accelerated by super time stepping method (Alexiades, Amiez & Gremaud 1996).

For this study, we newly implemented the Hall current term with standard smoothed particle hydrodynamics (SPH) discretization according to Wurster, Price & Ayliffe (2014). The Hall current term couples with the ideal magnetohydrodynamics (MHD) terms and changes the phase velocity. Thus, it is not clear that the sub-cycle method, which is often used for the resistive MHD terms (Machida & Matsumoto 2011; Tsukamoto et al. 2015a), is valid for the Hall current term. Therefore, in our simulations, the ideal MHD term and the Hall current term were updated simultaneously with the time-step of the Hall current term, $\Delta t_{\text{Hall}} = C_{\text{hall}} h^2 / (4\pi |\eta_{\text{H}}|)$ (Sano & Stone 2002). Here, C_{hall} is the Courant-Friedrichs-Levy (CFL) number for the Hall current term, and we adopted $C_{\text{hall}} = 0.4$. h is the smoothing length. Because of the additional cost due to the Hall current term, the total computational cost of the simulation with the non-ideal effect is more than 100 times higher than that of the simulation without the non-ideal effect. We conducted the numerical tests for the Hall current term. We confirmed that the scheme can correctly calculate the whistler mode in the linear wave propagation test. Furthermore, we conducted gravitational collapse test of non-rotating cloud cores and confirmed that the rotation amplitude induced by the Hall current term does not depend on the direction of the magnetic field. We adopted the equation of state (EOS) used in Tomida et al. (2013), The dust opacity table was adopted from Semenov et al. (2003) and the gas opacity table was from Ferguson et al. (2005). We employed resistivity table used in our previous works (Okuzumi 2009; Tsukamoto et al. 2015a) We modeled the initial cloud core with an isothermal uniform gas sphere. The initial cores are modeled with about 3×10^6 SPH particles. The parameters for the cloud core are also the same as that used in the previous study (Tsukamoto et al. 2015a) except for the number of the particles.

3 RESULTS

In figure 1, we show the structure at the center of the cloud core. The left two panels show the result of Model Para where the rotation vector is in the anti-parallel to the magnetic field vector. The right panels show that of Model Ortho

Table 1. The model names, the included non-ideal magnetic effects, and the relative angle between the initial magnetic field and the rotation vector θ of cloud core are shown. The initial mass and temperature of the parent cloud were fixed at $1 M_{\odot}$ and 10 K, respectively. Initially, the core has a radius of $R \sim 3.0 \times 10^3$ AU and is rigidly rotating with an angular velocity of $\Omega_0 = 2.2 \times 10^{-13} \text{ s}^{-1}$. The initial magnetic field was uniform and parallel to the rotation (z -) axis with a magnitude of $B_0 = 1.7 \times 10^2 \mu\text{G}$. The corresponding initial mass-to-flux ratio relative to the critical value is $\mu = (M/\Phi)/(M/\Phi)_{\text{crit}} = 4$ where $\Phi = \pi R^2 B_0$ and $(M/\Phi)_{\text{crit}} = (0.53/3\pi)(5/G)^{1/2}$. Here, “Included” (“Not included”) means that the corresponding non-ideal effect is (is not) included.

Model	Ohmic and ambipolar diffusion	Hall current term	θ
Para	Included	Included	180°
Ortho	Included	Included	0°
NoHall	Included	Not included	0°

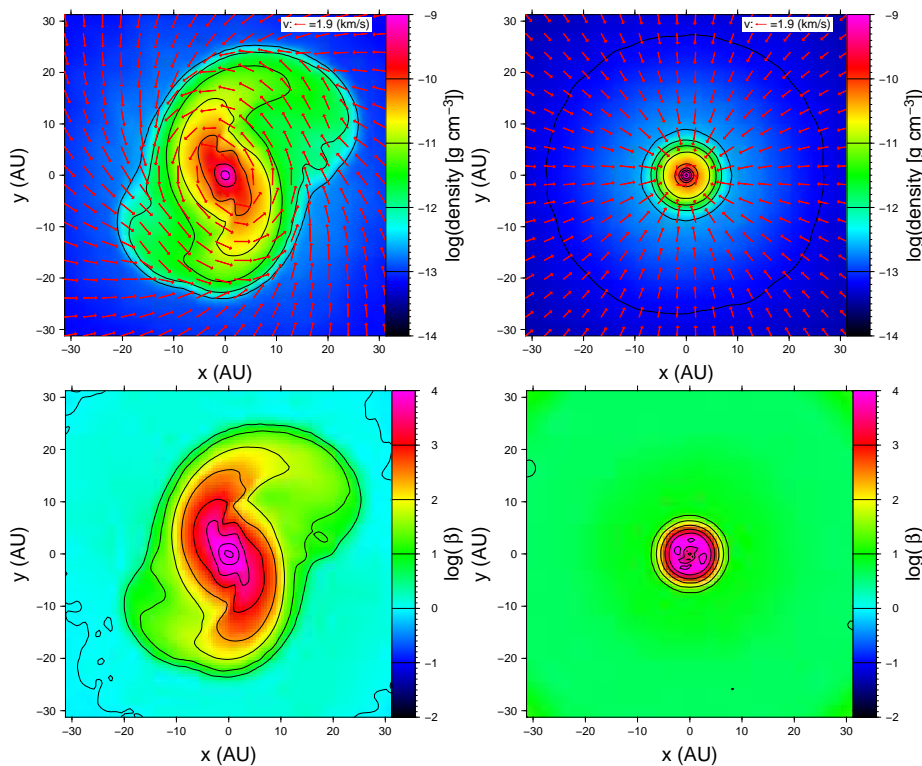


Figure 1. Cross sections of the density (top panels) and the plasma β (bottom panels) in the x-y plane. The left two panels show the result of Model Para where the rotation vector is in the anti-parallel to the mean magnetic field direction. The right panes show that of Model Ortho where rotation vector is parallel to the mean magnetic field. The central densities at these snapshots are $10^{-9} \text{ g cm}^{-3}$ for left panels which correspond to slightly before the protostar formation, and $10^{-2} \text{ g cm}^{-3}$ for right panels, immediately after the protostar formation.

where rotation vector is parallel to the magnetic field vector. The central densities at these snapshots are $10^{-9} \text{ g cm}^{-3}$ for left panels which correspond to slightly before the protostar formation, and $10^{-2} \text{ g cm}^{-3}$ for right panels, immediately after the protostar formation.

When the rotation vector and magnetic field are in the anti-parallel configuration, a large disk with a size of $r \sim 20$ AU is formed before the formation of the protostar (Model Para; top left panel). The disk is so massive that spiral arms are created by the gravitational instability. We confirmed that the Toomre’s Q value, $Q = \kappa_{\text{ep}} c_s / (\pi G \Sigma)$ is $Q \sim 1$ in the entire disk region ($5 \lesssim r \lesssim 20$ AU). In the top panel of figure 2, we show the the ratio of the sum of the centrifugal and the pressure gradient forces to the radial gravitational force with the solid line and the ratio of the centrifugal to

the radial gravitational force with the dashed line. This figure clearly shows that the gas is mainly supported by the centrifugal force. Therefore, a rotationally-supported massive disk is formed in Model Para. On the other hand, when the rotation vector and magnetic field are in the parallel configuration, no large disk ($r \gtrsim 10$ AU) appears (Model Ortho; top right panel of figure 1) because the magnetic braking is strengthened by the Hall current term and the angular momentum is efficiently removed from the central region. The dense region ($\rho > 10^{-11} \text{ g cm}^{-3}$) at the center which has a radius of $r \sim 5$ AU is the remnant of the first core and is not a rotationally-supported disk. Although a rotationally-supported disk with $r \lesssim 0.6$ AU is formed in Model Ortho around the protostar immediately after its formation as shown in the bottom panel of the figure 2, the

difference of the disk size of Model Para and Model Ortho is remarkable.

The plasma β in the disk regions ($r \lesssim 20$ AU) of Model Para are large ($\beta > 100$) because the rotationally supported dense disk extends over large radius where the magnetic diffusion is effective and the magnetic flux is largely removed from the regions. In the high β regions, the magnetic braking is no longer important. On the other hand, the disk is sufficiently massive and develops gravitational instability. Thus, gravitational instability plays a crucial role for angular momentum transfer in the early evolutionary phase. Furthermore, in such a massive extended disk, disk fragmentation which is a promising mechanism for the formation of binaries or wide-orbit planets (Marois et al. 2010) possibly occurs in the subsequent evolution (Boss 1997; Inutsuka, Machida & Matsumoto 2010; Machida, Inutsuka & Matsumoto 2011; Tsukamoto & Machida 2011, 2013; Tsukamoto, Machida & Inutsuka 2013; Tsukamoto et al. 2015b). Thus, the parallel or anti-parallel property of the cloud core should play a crucial role for the formation process of the binary or wide-orbit planets.

To quantify the strength of the rotation at the center of the cloud core, we show the mean specific angular momentum of regions with $\rho > 10^{13}$ g cm $^{-3}$ as a function of the central density in figure 3. The central density monotonically increases with time. Therefore, this figure shows the time evolution of the angular momentum of the central region. The figure shows that the specific angular momentum in anti-parallel case is about an order of magnitude larger than that of the parallel case. The specific angular momentum of the simulation with the Hall current term and parallel (anti-parallel) magnetic field is about three times smaller (larger) than that of the simulation without the Hall current term (Model NoHall). The combination of the spin-up effect in the anti-parallel case and the spin-down effect in the parallel case causes the large difference.

Because of the conservation of angular momentum, the spin-up due to the Hall term at the center causes spin-down, and eventually, anti-rotation of the outer region against the disk. In figure 4, we show the cross section of the rotation velocity distribution in the $x - z$ plane at the same epoch of figure 1. This figure clearly shows an anti-rotating envelope which surrounds the forward rotating inner region. The anti-rotating envelope has a scale of ~ 200 AU and a rotation velocity of ~ 1 km at the end of the simulation. Since the anti-rotation of envelope are driven by torsional Alfvén waves, anti-rotating region expands with time and will propagate to the outside of the parental molecular cloud core. Thus, the angular momentum of which direction is opposite to the disk is eventually cast away to the interstellar medium. We predict future observations will find the presence of an anti-rotating envelope against disk rotation in the Class 0 YSOs. These observation would provide clear evidence for our findings that the Hall current term plays an important role in the formation and evolution of circumstellar disks.

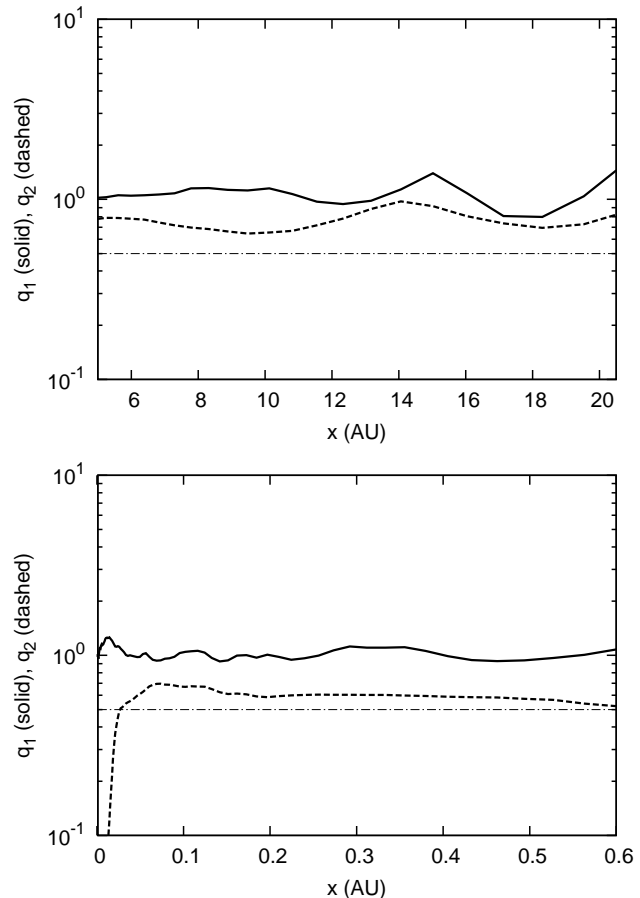


Figure 2. Solid lines show the ratio of the sum of the centrifugal force and the pressure gradient force to the radial gravitational force, $q_1 = \left| \frac{v_\phi^2/x + \nabla_r p/\rho}{\nabla_r \Phi} \right|$, as a function of the radius. Here, v_ϕ , p , and Φ are the rotation velocity, gas pressure, and the gravitational potential, respectively. Dashed lines show the ratio of the centrifugal force to the radial gravitational force, $q_2 = \left| \frac{v_\phi^2/x}{\nabla_r \Phi} \right|$. Dashed-dotted lines show $q = 0.5$. In the regions where the dashed lines are larger than the dashed-dotted lines, the gas is mainly supported by the centrifugal force. The top and bottom panels show the results of model Para and model Ortho, respectively. The epochs of each model are the same as in figure 1.

4 CONCLUSIONS AND DISCUSSION

In this study, we investigated the effect of the Hall current term on the formation of circumstellar disk using simulations starting from prestellar cloud core. In our simulations, all non-ideal effects as well as the radiation transfer are considered. To our knowledge, this is the first study that simultaneously includes these physical processes in a three-dimensional simulation.

We found that the disk evolution can be categorized into two cases according to an inherent property of the cloud core, whether the initial magnetic field and the rotation vector are parallel or anti-parallel. When the rotational vector and the magnetic field have an anti-parallel configuration, a relatively large ($r \gtrsim 10$ AU) and massive disk forms simultaneously with the protostar formation. On the other hand, a disk with $r \gtrsim 1$ AU does not form when the rotational vector and the magnetic field are parallel. In this way, the parity of

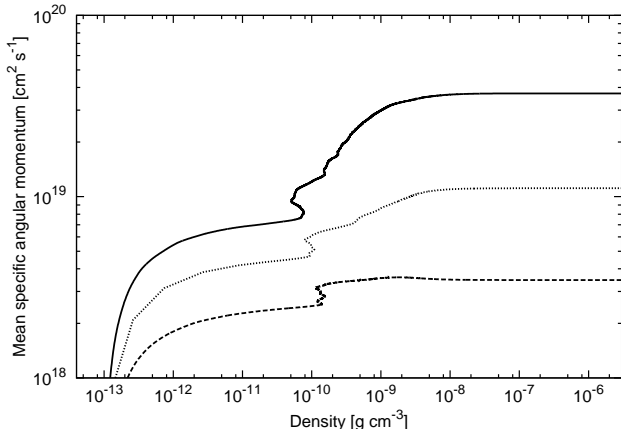


Figure 3. The time evolution of the mean specific angular momentum of the inner region with $\rho > 10^{-13} \text{ g cm}^{-3}$ as a function of the central density. The solid, dashed, and dotted lines show the results of Model Para, Ortho, and NoHall, respectively.

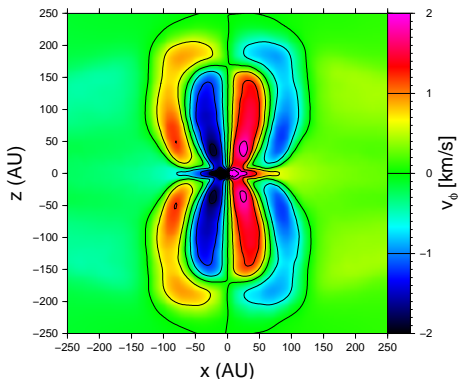


Figure 4. The cross section of the distribution of v_y in the x - z plane in Model Para. The epoch of the snapshot is the same as that in Fig. 1.

the magnetic field direction changes the disk formation process significantly, which has not been paid much attention to so far. Since the parallel and anti-parallel properties are inherent and do not readily change in time, we expect that the spin-up and spin-down effect due to the Hall current term are also important in the subsequent disk evolution and the difference between the two cases is maintained or enhanced. Therefore, we suggest that the disk evolution can be categorized into two cases. We may call the resultant parallel and anti-parallel systems as *ortho*-YSOs and *para*-YSOs, respectively.

Our results predict that the bimodality in the disk size distribution spontaneously arises due to the Hall current term in typically magnetized molecular clouds. We tend to think that the disk size has a unimodal distribution according to the strength of the rotation and the magnetic field of the cloud cores. However, as we have shown above, the hall term changes the disk size according to the inherent parallel or anti-parallel property of the cores. It is expected that almost half of the molecular cloud cores have the parallel configuration and the others have the anti-parallel configuration because the Hall term would not play the role during the cloud core formation (Wardle 2004) and there is

no physical mechanism which distinguishes the parallel and anti-parallel configurations. On the other hand, during the gravitational collapse of cloud core, the Hall term becomes effective and decreases or increases the gas rotation according to the parallel and anti-parallel property. Therefore, the bimodality of the disk size distribution would spontaneously arise from the unimodal distributions of the rotation and the magnetic field strength of the cores. As we have pointed out, the recent observation of the Class 0 YSOs (Tobin et al. 2015) showed that almost half of the YSOs they observed have the signature of the relatively large disk, while the others do not show the signature of disk. Yen et al. (2015) also found that some Class 0 YSOs do not show any signature of a disk with a size of $r > 10 \text{ AU}$. These observations seem to support our findings. Of course, more observations of YSOs with kinematic informations are required to confirm our prediction.

An observational signature predicted from our results is the anti-rotating envelope in the Class 0 YSOs. The envelope was found to be anti-rotating against the rotational direction of the disk in the anti-parallel case. At the end of the simulations, the anti-rotating envelope had a size of $r \gtrsim 100 \text{ AU}$ and the rotation velocity of $v_\phi \sim 1 \text{ km}$. Because the anti-rotation of envelope are stem from torsional Alfvén waves, anti-rotating region expands with time. We predict future observations will find the presence of an anti-rotating envelope against disk rotation in the Class 0 YSOs. These observation would provide clear evidence for our findings that the Hall current term plays an important role in the formation and evolution of circumstellar disks.

In this paper, several simplifications were adopted and their influences should be investigated in future works. We employed a fixed dust grain size of $a = 0.035 \mu\text{m}$. The magnetic resistivity are sensitive to the dust size and the dust models. Thus, the simulations with different dust size and model such as MRN dust distribution (Mathis, Rumpl & Nordsieck 1977) are necessary to confirm our results. The misalignment between the magnetic field and the rotation vector is another important issue. In our simulations, the initial rotation vector and the magnetic field are in perfectly parallel or anti-parallel configurations. However, it is expected that they are mutually misaligned in the realistic cloud cores. Joos, Hennebelle & Ciardi (2012) proposed that the misalignment between the magnetic field and the rotation vector weakens the magnetic braking. Although the resultant mean specific angular momentum differs only by a factor of two to three (see their Fig. 4) in ideal MHD limit, the misalignment may play an important role when the non-ideal MHD effects are included.

ACKNOWLEDGMENTS

We thank K. Tomida and Y. Hori for providing EOS table. The computations were performed on the XC30 system at CfCA of NAOJ.

REFERENCES

Alexiades V., Amiez G., Gremaud P.-A., 1996, Com. Num. Meth. Eng, 12, 12

- Bate M. R., 1998, *ApJ*, 508, L95
- Bate M. R., Tricco T. S., Price D. J., 2014, *MNRAS*, 437, 77
- Boss A. P., 1997, *Science*, 276, 1836
- Braiding C. R., Wardle M., 2012, *MNRAS*, 422, 261
- Dapp W. B., Basu S., Kunz M. W., 2012, *A&A*, 541, A35
- Ferguson J. W., Alexander D. R., Allard F., Barman T., Bodnarik J. G., Hauschildt P. H., Heffner-Wong A., Tamanai A., 2005, *ApJ*, 623, 585
- Goodman A. A., Benson P. J., Fuller G. A., Myers P. C., 1993, *ApJ*, 406, 528
- Hennebelle P., Fromang S., 2008, *A&A*, 477, 9
- Inutsuka S., Machida M. N., Matsumoto T., 2010, *ApJ*, 718, L58
- Iwasaki K., Inutsuka S., 2011, *MNRAS*, 418, 1668
- Iwasaki K., Inutsuka S.-I., 2013, in *Astronomical Society of the Pacific Conference Series*, Vol. 474, *Numerical Modeling of Space Plasma Flows (ASTRONUM2012)*, Pogorelov N. V., Audit E., Zank G. P., eds., p. 239
- Joos M., Hennebelle P., Ciardi A., 2012, *A&A*, 543, A128
- Krasnopolsky R., Li Z.-Y., Shang H., 2011, *ApJ*, 733, 54
- Li Z.-Y., Krasnopolsky R., Shang H., 2011, *ApJ*, 738, 180
- Machida M. N., Inutsuka S., Matsumoto T., 2011, *ApJ*, 729, 42
- Machida M. N., Inutsuka S.-i., Matsumoto T., 2014, *MNRAS*, 438, 2278
- Machida M. N., Matsumoto T., 2011, *MNRAS*, 413, 2767
- Marois C., Zuckerman B., Konopacky Q. M., Macintosh B., Barman T., 2010, *Nature*, 468, 1080
- Mathis J. S., Rimpl W., Nordsieck K. H., 1977, *ApJ*, 217, 425
- Mellon R. R., Li Z.-Y., 2008, *ApJ*, 681, 1356
- , 2009, *ApJ*, 698, 922
- Mouschovias T. C., Paleologou E. V., 1979, *ApJ*, 230, 204
- Ohashi N. et al., 2014, *ApJ*, 796, 131
- Okuzumi S., 2009, *ApJ*, 698, 1122
- Sakai N. et al., 2014, *Nature*, 507, 78
- Sano T., Stone J. M., 2002, *ApJ*, 570, 314
- Semenov D., Henning T., Helling C., Ilgner M., Sedlmayr E., 2003, *A&A*, 410, 611
- Tobin J. J. et al., 2015, *ArXiv e-prints*
- Tomida K., Okuzumi S., Machida M. N., 2015, *ApJ*, 801, 117
- Tomida K., Tomisaka K., Matsumoto T., Hori Y., Okuzumi S., Machida M. N., Saigo K., 2013, *ApJ*, 763, 6
- Troland T. H., Crutcher R. M., 2008, *ApJ*, 680, 457
- Tsukamoto Y., Iwasaki K., Inutsuka S.-i., 2013, *MNRAS*, 434, 2593
- Tsukamoto Y., Iwasaki K., Okuzumi S., Machida M. N., Inutsuka S.-i., 2015a, *ArXiv e-prints*
- Tsukamoto Y., Machida M. N., 2011, *MNRAS*, 416, 591
- , 2013, *MNRAS*, 428, 1321
- Tsukamoto Y., Machida M. N., Inutsuka S., 2013, *MNRAS*, 436, 1667
- Tsukamoto Y., Takahashi S. Z., Machida M. N., Inutsuka S., 2015b, *MNRAS*, 446, 1175
- Wardle M., 2004, *Ap&SS*, 292, 317
- Wardle M., Ng C., 1999, *MNRAS*, 303, 239
- Whitehouse S. C., Bate M. R., 2004, *MNRAS*, 353, 1078
- Whitehouse S. C., Bate M. R., Monaghan J. J., 2005, *MNRAS*, 364, 1367
- Wurster J., Price D., Ayliffe B., 2014, *MNRAS*, 444, 1104
- Yen H.-W., Koch P. M., Takakuwa S., Ho P. T. P., Ohashi N., Tang Y.-W., 2015, *ApJ*, 799, 193